Immunochemical approaches to monitor and modulate the adaptive immune system

Luimstra, J.J.

2

Altered peptide ligands revisited: vaccine design through chemically modified HLA-A2-restricted T cell epitopes

Rieuwert Hoppes[1*], Rimke Oostvogels[2,3*], Jolien J. Luimstra[1], Kim Wals[1], Mireille Toebes[4], Laura Bies[4], Reggy Ekkebus[1], Pramila Rijal[1], Patrick H.N. Celie[5], Julie H. Huang[2], Maarten E. Emmelot[2], Robbert M. Spaapen[1], Henk Lokhorst[3], Ton N. M. Schumacher[4], Tuna Mutis[2], Boris Rodenko[1,6], and Huib Ovaa[1]

*R. Hoppes and R. Oostvogels contributed equally to this work.

[1]Division of Cell Biology, The Netherlands Cancer Institute, Amsterdam, The Netherlands
[2]Department of Clinical Chemistry and Haematology, University Medical Center Utrecht, Utrecht, The Netherlands
[3]Department of Haematology, University Medical Center Utrecht, Utrecht, The Netherlands
[4]Division of Immunology, The Netherlands Cancer Institute, Amsterdam, The Netherlands
[5]Division of Biochemistry, The Netherlands Cancer Institute, Amsterdam, The Netherlands
[6]Institute of Infection, Immunity and Inflammation, University of Glasgow, Glasgow, United Kingdom

Journal of Immunology 193, 4803-4813 (2014)

Abstract

Virus or tumor Ag-derived peptides that are displayed by MHC class I molecules are attractive starting points for vaccine development a they induce strong protective and therapeutic cytotoxic T cell responses. In thus study, we show that the MHC binding and consequent T cell reactivity against several HLA-A*02:01-restricted epitopes can be further improved through the incorporation of non-proteogenic amino acids at primary and secondary anchor positions. We screened more than 90 non-proteogenic, synthetic amino acids through a range of epitopes and tested more than 3000 chemically enhanced altered peptide ligands (CPLs) for binding affinity to HLA-A*02:01. With this approach, we designed CPLs of viral epitopes, of melanoma-associated Ags, and of the minor histocompatibility Ag UTA2-1, which is currently being evaluated for its antileukemic activity in clinical dendritic cell vaccination trials. The crystal structure of one of the CPLs in complex with HLA-A*02:01 revealed the molecular interactions likely responsible for improved binding. The best CPLs displayed enhanced affinity for MHC, increasing MHC stability and prolonging recognition by Ag-specific T cells and, most importantly, they induced accelerated expansion of antitumor T cell frequencies in vitro and in vivo as compared with the native epitope. Eventually, we were able to construct a toolbox of preferred non-proteogenic residues with which practically any given HLA-A*02:01-restricted epitope can be readily optimized. These CPLs could improve the therapeutic outcome of vaccination strategies or can be used for ex vivo enrichment and faster expansion of Ag-specific T cells for transfer into patients.

Introduction

In the treatment of cancer and the prevention of infectious diseases, the use of therapeutic or prophylactic peptide vaccines can be a successful method to specifically direct the immune system against the right targets. The peptides administered to the patient mimic the epitopes presented on the target cells when associated with the restricting MHC and would thus be capable of inducing relevant immune responses.

For immunotherapy of cancer, various clinical applications in the past decades provided ample evidence of the feasibility, safety, and immunogenicity of this type of vaccine; however, the efficacy has mostly been limited[1,2]. Many variables in the design of peptide vaccination, such as type and length of the peptides, loading of one or multiple peptides on APCs or route of administration could potentially attribute to these disappointing observations. Selecting the right epitope is a crucial step in the design of an effective vaccine. Obviously, the

vaccine peptide needs to be presented on the targeted tumor cells at sufficient expression levels, but also peptide-MHC affinity appears to be a decisive factor for the immunogenic potential[3-7]. Recent research suggests that high-peptide MHC affinities of targeted epitopes are required for complete tumor eradication and tumor stroma destruction by specific T cells, presumably through the formation of stable synapses between the APCs and the effector T cells that are necessary for optimal stimulation of the latter[6]. In addition, the half-life of peptide-MHC (pMHC) complexes has been directly correlated to immunogenicity[8], and extension of the duration of the peptide-MHC interaction (and consequent dwell time on the cell surface) may therefore lead to more effective peptide vaccines by the induction of higher frequencies of epitope-specific T cells[9].

A frequent problem with peptide vaccinations until now is the low immunogenicity of the tumor-associated Ags used, which are usually derived from self-proteins. Because of thymic selection processes, the T cell repertoire is mainly shaped to recognize foreign Ags with high affinity in contrast to peptides derived from self-proteins[10]. To circumvent these issues, the replacement of amino acids in so-called anchor positions that contribute significantly to MHC affinity has been proposed. Epitopes modified based on amino acid substitutions are termed "altered peptide ligands" (APLs)[11]. A well-known example of such an APL is the alanine to leucine modification in the melanoma-associated Mart-1/Melan-A_{26-35} epitope EAAGIGILTV that leads to enhanced MHC-binding[12].

In general, MHC class I molecules accommodate peptides of 8-10 aas long that contain preferred MHC allele-specific residues on anchor positions (Fig. 1A)[13]. The affinity of a peptide for an MHC molecule is determined by the potential of these anchor residues to form stable molecular interactions with the MHC allele-specific pockets, depending on their shape, size, and electrostatic complementarity with proximal MHC residues[14,15]. The exact localization of the anchor residues depends on the MHC allele, but they are mainly in close proximity to the N- and C-termini of bound peptides[13,16]. In contrast, interaction with the TCRs of cytotoxic T cells heavily relies on the middle part of the peptide that extrudes out of the MHC binding groove[8,10]. Therefore, modifications aimed at increasing an epitope's affinity for MHC molecules are in principle restricted to positions near the N- and C-termini to ensure retained immunogenicity. Anchor substitutions have been introduced successfully within peptides to improve MHC class I binding and to enhance TCR activation[12,17-19]. Substitutions in the TCR interacting region, however, frequently result in heteroclitic analogs that can lead to hyperstimulation of the CTL, achieving occasionally a more potent immune response compared with the native epitope; far more often, they will cause T cell exhaustion or lead to an abrogated TCR interaction[20-22].

Synthetic engineering of peptide epitopes may confer beneficial properties to the peptide vaccine, such as improved MHC class I binding, protease resistance,

and enhanced bioavailability. Strategies that have been pursued to improve and stabilize MHC epitopes include the incorporation of residues such as nonencoded α-amino acids[23-25], photoreactive cross-linking amino acids[26], N-methylated amino acids[27] and β-amino acids[27-30], backbone reduction (reviewed in Ref. 31), (partial) retroinversion by using D-amino acids[32,33], N-terminal methylation and C-terminal amidation[27,34] and pegylation (reviewed in Ref. 35). The majority of these modifications are aimed at improving the biostability of peptide Ags, often at the cost of losing MHC affinity, immunogenicity, or both. The limited rate of success in epitope improvement might be found in the often small set of non-natural amino acids used to generate primarily monosubstituted peptide analogs. In this study, we aimed to address this issue by systematically introducing multiple substitutions in cognate Ags using a large set of synthetic amino acids. Our approach involves the replacement of primary and secondary anchor residues of known T cell epitopes with non-proteogenic amino acids (Fig. 1, A and B). The resulting non-natural peptides will be referred to as "chemically enhanced altered peptide ligands" (CPLs) as opposed to the "classical" APLs containing only proteogenic amino acid substitutions. To define the best CPLs, we modified 12 well-known T cell epitopes with more than 90 different non-proteogenic amino acids and tested 3000 peptides in total. We focused on replacing amino acids on positions close to the N- and C-termini as we aimed to improve the HLA affinity of several model epitopes without interfering with TCR recognition. For our optimization studies, we selected epitopes restricted to HLA-A*02:01, because this allele is the most abundant MHC molecule in humans of Caucasian origin.

We first used several viral epitopes and tumor-associated Ags as model peptides to test this principle. For our final experiments, we modified the recently identified minor histocompatibility Ag (mHag) UTA2-1[36]. This HLA-A*02:01-restricted Ag, because of its sole expression in hematopoietic cells, is highly relevant for the therapy of relapsed lymphoid and myeloid malignancies of the hematopoietic system after allogeneic stem-cell transplantation. UTA2-1 is currently included in clinical trials in which patients who are not responding to donor lymphocyte infusions are treated with mHag-loaded dendritic cell vaccinations.

We show that the substitution of amino acids at anchoring positions by particular non-proteogenic amino acids led to superior MHC binding in comparison with substitution with proteogenic amino acids, with concomitant improvement of the immunogenicity of these epitopes. For the immunotherapeutic mHag UTA2-1, we were able to design a CPL that in vitro and in vivo evoked significantly enhanced proliferation of UTA2-1-specific T cells. Moreover, the cytotoxic capacity of these T cells against targets expressing the natural UTA2-1 Ag was maintained, confirming the relevance of this approach for use in clinical practice.

Results

Enhancing epitope binding affinity by substitutions with non-proteogenic amino acid residues

To test our model and to attempt to enhance peptide binding to HLA-A*02:01by amino acid substitutions in the epitope, we first set out to improve the affinity of two well-known viral epitopes: Influenza Matrix 1_{58-66} epitope GILGFVFTL[37], as a stringent model epitope already having high affinity for HLA-A*02:01, and CMV $pp65_{495-503}$ peptide NLVPMVATV[38] as an intermediate model peptide having a moderate affinity for HLA-A*02:01[39]. To explore the general scope of substitutions with proteogenic amino acids, we systematically introduced all 20 proteogenic residues on all nine positions in the peptides and screened these peptides for binding capacity to HLA-A*02:01 using an MHC exchange fluorescence polarization FP assay (Table S1)[40]. Using proteogenic amino acid substitutions the HLA binding score (defined as the percent inhibition of FP tracer peptide binding) could maximally be raised from 36% for the native NLVPMVATV peptide to 70% for its related APLs and from 76% for the native GILGFVFTL peptide to 87% for the corresponding APLs. It should, however, be noted that these substitutions include those that are part of the TCR interacting region (Fig. 1A) and hence could affect TCR binding and selectivity. Having observed that specific substitutions with proteogenic amino acids can lead to enhanced binding affinity, we proceeded to further increase peptide-MHC affinity through the introduction of non-proteogenic amino acids, including the D-enantiomers of proteogenic amino acids. Making full use of the possibilities of medicinal chemistry to optimize ligand-protein interactions, we incorporated 90 non-proteogenic amino acid derivatives on the positions indicated in Figure 1A in GILGFVFTL and NLVPMVATV, leading to monosubstituted, disubstituted, and trisubstituted CPLs, and we determined the HLA binding scores of the resulting set of 500 peptides (Fig. 1C).

Several non-proteogenic residues revealed further enhancement of affinity relative to the substitutions with proteogenic amino acids. In particular, the introduction of D-α-methyl-phenylglycine (am-phg) on P_1 generally led to additional improvements in HLA binding, as seen for CPLs [am-phg][NVA]LGFV[4-FPHE]TL and [am-phg][CpALA]LGFV[4-FPHE]TL with HLA binding scores of 96% and 97%, respectively, as compared with 87% for the best APL GILGFVFPL. By introducing L-2-amino-octanoic acid (2-AOC) on P_3 of the NLVPMVATV peptide the HLA binding score was increased up to 73%. A frequent improvement was observed by the introduction of 4-fluorophenylalanine (4-FPHE) on P_{C-2}, a non-anchor position (Fig. 1, A and B). By performing similar screens through five other viral epitopes (Fig. S1), we learned which non-proteogenic amino acid substitutions frequently led to enhancement of HLA affinity, allowing us to compose a list of preferred residues (Fig. 1B). Functional assays with several donor-derived

GILGFVFTL-positive CD8+ T cell clones showed that CPLs with substitutions on P_1, P_2, and P_{C-2} and P_C were generally able to (hyper)stimulate CTLs, but CPLs with modifications on P_3 gave variable results (data not shown).

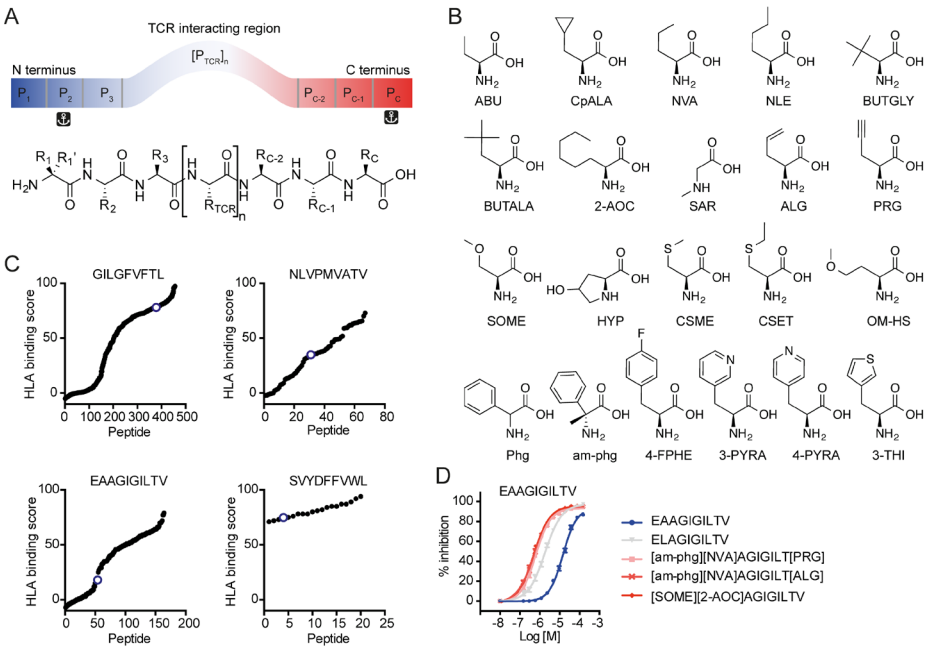

Figure 1. **Introduction of nonproteogenic amino acids leads to CPLs with higher HLA affinity than their respective index peptides.** (A) Schematic representation of amino acid positions of an HLA-A*02:01-restricted epitope. Positions P_1 to P_3 and P_{C-2} to P_C have been modified in this study, resulting in modified side chain substituents $R_{1,1}$, R_2, R_3, and R_{C-2}, R_{C-1}, and R_C. Positions P_{TCR} were left untouched to retain interaction with the TCR. P_2 and P_C anchor residues are indicated. (B) Structures of preferred non-proteogenic amino acid residues leading to enhanced HLA affinity that emerged from screening 90 different amino acid residues in 20 epitopes. L-α-Amino acids are in all upper case, and D-amino acids are in sentence case. Phg denotes a racemic mixture of DL-phenylglycine. In peptide sequences, non-proteogenic residues are enclosed in brackets. (C) Screening CPLs for HLA affinity was performed with a competitive HLA-A*02:01 ultraviolet exchange fluorescence polarization assay. HLA binding scores are the percent inhibition of FP tracer peptide binding. Each data point (•) represents a different CPL of the indicated parent epitope, accommodating one, two, or three non-proteogenic amino acid substitutions. Scores for parent epitopes are indicated by (○) and include influenza A matrix $1_{58–66}$ GILGFVFTL, CMV pp65$_{495–503}$ NLVPMVATV, melanoma Mart-$1_{26–35}$ EAAGIGILTV, and melanoma Trp-$2_{180–188}$ SVYDFFVWL. See Figure S1 for optimization of additional epitopes. (D) For the strongest binders, IC50 values were determined showing that Mart-$1_{26–35}$-based CPLs display an increase in HLA affinity by two orders of magnitude (see also Table 2).

Optimization of the HLA affinity of tumor epitopes

After showing proof of principle for improving the HLA affinity of even highly affine and immunogenic viral epitopes by incorporation of synthetic amino acids, we aimed to optimize melanoma-associated epitopes, which typically display low MHC affinity and hence low immunogenicity[8]. The HLA-A*02:01-restricted Melan-A/Mart-1 epitope EAAGIGILTV[41] has very low affinity for HLA-A*02:01, practically precluding its use in immunologic applications such as pMHC multimer staining and T cell isolation. The low MHC affinity is primarily due to the suboptimal anchor residue, alanine, on P_2, and substitution of this residue for the preferred anchor residue leucine (A2L) has been reported to enhance HLA binding[12] and has become a benchmark example of an APL facilitating the

Table 1. **Data collection and refinement statistics.**

HLA-A*02:01::[am-phg][NVA]AGIGILT[PRG][a]	
Data collection	
Space group	$P2_1$
Cell dimensions	
a, *b*, *c* (Å)	63.18, 87.14, 79.19
A, β, γ (°)	90.00, 90.15, 90.00
Resolution (Å)	40.00–1.65 (1.74–1.65)[b]
R_{sym} or R_{merge}	4.1 (48.3)
$I/\sigma I$	13.2 (1.6)
Completeness (%)	99.6 (99.8)
Redundancy	3.4 (3.5)
Refinement	
Resolution (Å)	20.00–1.65
No. of reflections	97482
R_{work}/R_{free}	15.6/17.9
Twinning	2 domains
Twin domain 1 fraction	0.748
Twin domain 1 operator	H, K, L
Twin domain 2 fraction	0.252
Twin domain 2 operator	-H, -K, -L
No. of atoms	
Protein	6851
Ligand/ion	78
Water	540
B-factors	
Protein	14.1
Ligand/ion	45.3
Water	31.8
R.m.s. deviations	
Bond lengths (Å)	0.012
Bond angles (°)	1.563

X-ray diffraction data were collected on one single crystal. [a]The crystal structure presented in this article has been submitted to the RCSB Protein Data Bank (http://www.rcsb.org/pdb/home/home.do) under identification code 4WJ5. [b]Values in parentheses are for highest-resolution shell.

Table 2. **MHC binding, TCR recognition, and T cell activating ability of chemically optimized melanoma epitopes.**

Sequence	MHC Binding (μM ± SEM)[a]	% pMHC multimer$^+$ CTLs[b]	% IFN-γ$^+$ CTLs[c] 1 h	% IFN-γ$^+$ CTLs[c] 24 h	Literature reference
EAAGIGILTV—Mart-1$_{(26–35)}$	14.56 ± 0.3	6.4 ± 0.4	43 ± 16	0 ± 0	(53)
ELAGIGILTV	1.9 ± 0.10	5.6 ± 0.4	79 ± 7	30 ± 7	(12)
[am-phg][2-AOC]AGIGILT[PRG]	0.26 ± 0.03	5.6 ± 0.5	ND	ND	
[am-phg][NLE]AGIGILT[PRG]	0.4 ± 0.01	6.0 ± 0.3	82 ± 7	49 ± 8	
[am-phg][NVA]AGIGILT[ALG]	0.41 ± 0.10	5.1 ± 0.3	86 ± 4	69 ± 6	
[am-phg][NVA]AGIGILT[PRG]	0.51 ± 0.01	6.3 ± 0.1	81 ± 7	56 ± 12	
[am-phg]LAGIGILT[PRG]	0.48 ± 0.02	5.6 ± 0.2	77 ± 7	56 ± 14	
[CSME][2-AOC]AGIGILT[PRG]	0.51 ± 0.08	5.1 ± 0.3	84 ± 6	62 ± 7	
[CSME][2-AOC]AGIGILTV	0.47 ± 0.08	6.5 ± 0.3	78 ± 7	67 ± 12	
[CSME][NLE]AGIGILTV	0.97 ± 0.06	6.1 ± 0.1	76 ± 6	60 ± 12	
[CSME][NVA]AGIGILTV	0.87 ± 0.05	6.8 ± 0.4	78 ± 5	57 ± 15	
[CSME]LAGIGILT[PRG]	1.13 ± 0.07	5.1 ± 0.1	78 ± 7	57 ± 11	
[CSME]LAGIGILTV	1.36 ± 0.03	7.3 ± 0.5	73 ± 13	52 ± 13	
[SOME][2-AOC]AGIGILTV	0.22 ± 0.03	5.1 ± 0.2	72 ± 3	66 ± 11	
[SOME]LAGIGILTV	1.13 ± 0.06	4.8 ± 0	84 ± 2	66 ± 4	
SVYDFFVWL—Trp-2$_{(180–188)}$	0.76 ± 0.15		48 ± 3	30 ± 7	(54)
[am-phg][2-AOC]YDFFVW[PRG]	0.51 ± 0.1		37 ± 5	0 ± 0	
[am-phg][2-AOC]YDFFVWL	0.71 ± 0.09		62 ± 2	56 ± 5	
[am-phg][CpALA]YDFFVW[PRG]	0.46 ± 0.08		50 ± 3	8 ± 1	
[am-phg][NVA]YDFFVW[PRG]	0.71 ± 0.09		54 ± 6	52 ± 2	
[am-phg][NVA]YDFFVWL	0.65 ± 0.08		75 ± 0	77 ± 1	
[CSME][2-AOC]YDFFVW[ALG]	0.52 ± 0.04				
[CSME][2-AOC]YDFFVWL	0.41 ± 0.1		59 ± 3	62 ± 3	
[CSME][CpALA]YDFFVW[PRG]	0.94 ± 0.11				
[CSME][NVA]YDFFVW[PRG]	0.67 ± 0.14		20 ± 6	28 ± 4	
[Phg][2-AOC]YDFFVWL	0.51 ± 0.02		54 ± 3	66 ± 3	
[Phg][CpALA]YDFFVW[PRG]	0.80 ± 0.08		34 ± 6	46 ± 2	
[PHG][CpALA]YDFFVWL	0.60 ± 0.09		56 ± 3	62 ± 3	
[Phg][NVA]YDFFVW[ALG]	0.57 ± 0.05		42 ± 11	57 ± 4	
[Phg][NVA]YDFFVW[PRG]	0.74 ± 0.07		27 ± 8	29 ± 2	
[Phg][NVA]YDFFVWL	0.57 ± 0.1		58 ± 4	64 ± 5	
RLGPTLMCL—MG-50$_{(1243–1251)}$	1.78 ± 0.65				(55)
[am-phg][2-AOC]GPTLMC[PRG]	1.69 ± 0.57				
[am-phg][2-AOC]GPTLMCL	1.05 ± 0.05				
[am-phg][CpALA]GPTLMC[PRG]	1.03 ± 0.19				
[am-phg][CpALA]GPTLMCL	1.05 ± 0.12				
[CSME][2-AOC]GPTLMC[PRG]	1.01 ± 0.3				
[CSME][2-AOC]GPTLMCL	0.46 ± 0.03				
[CSME][CpALA]GPTLMCL	0.95 ± 0.07				
[CSME][NVA]GPTLMC[PRG]	0.79 ± 0.2				
[CSME][NVA]GPTLMCL	0.86 ± 0.04				
[Phg][2-AOC]GPTLMC[PRG]	0.63 ± 0.01				
[Phg][2-AOC]GPTLMCL	0.40 ± 0.07				
[Phg][CpALA]GPTLMC[PRG]	0.62 ± 0.19				
[Phg][CpALA]GPTLMCL	0.87 ± 0.08				
[Phg][NVA]GPTLMC[PRG]	0.73 ± 0.15				
[Phg][NVA]GPTLMCL	0.93 ± 0.42				
LLFGLALIEV—Mage-C2$_{(191–200)}$	47% (50%)[d]			11.5	(56)
[Phg][2-AOC]FGLALIEV	81% (81%)[d]			13.7	

[a]IC50 values were determined by an MHC exchange FP assay with peptide concentrations ranging from 100 mM to 50 nM. Values are the average of at least three biological replicates. SEM is standard error of means. [b]TCR interaction was measured by pMHC multimer staining of EAAGIGILTV selective CTLs. [c]T cell activation is represented by the percentage of IFN-γ-producing CD8$^+$ T cells specific for EAAGIGILTV (top half) or SVYDFFVWL (bottom half) upon coincubation with T2 APCs 1 or 24 h after pulsing the APCs with wild-type or modified epitopes. Values are the average of at least three independent experiments ± SE of means. [d]Values are HLA binding scores at 24 h as described in Materials and Methods. Value in parenthesis determined at 4 h.

study of Melan-A/Mart-1 CTL responses. To enhance MHC affinity further, we scanned non-proteogenic amino acids through this benchmark epitope. After synthesizing a set of 164 variants of the EAAGIGILTV peptide, we measured their HLA binding score (Fig. 1C) and then selected the 13 highest scoring CPLs and determined their IC50 value for binding to HLA-A*02:01 (Fig. 1D and Table 2). The introduction of multiple non-proteogenic amino acid residues in EAAGIGILTV yielded CPLs with an IC50 value of up to two orders of magnitude lower than displayed by the native epitope and one order of magnitude lower than displayed by the benchmark A2L APL. Using only the limited set of preferred residues shown in Figure 1B allowed us to reduce the number of peptide variants to be synthesized and screened to arrive at CPLs with improved HLA affinity. In this way we were readily able to optimize the affinity of melanoma Trp-$2_{180\text{-}188}$ epitope SVYDFFVWL[42] (Fig. 1C) and seven other melanoma epitopes: RLGPTLMCL ($MG50_{1243\text{-}1251}$)[43], LLFGLALIEV (Mage-$C2_{191\text{-}200}$), ALKDVEERV (Mage-$C2_{336\text{-}344}$), VIWEVLNAV (Mage-C2 $HCA587_{248\text{-}256}$), GLYDGMEHL (Mage-$A10_{254\text{-}262}$), YLEPGPVTA (pmel17/$gp100_{256\text{-}264}$) and VYDFFVWLHY (Trp-$2_{181\text{-}190}$) (Fig. S1). For the variants of SVYDFFVWL and RLGPTLMCL, we further determined their IC50 value for HLA-A*02:01 binding, and significant improvements were observed as these CPLs displayed 224-fold lower IC50 values than did the native epitopes (Table 2). In general, preferred modifications on P_1 included am-phg, O-methyl-L-serine (SOME) and S-methyl-L-serine (CSME), and L/D-(racemic) phenylglycine (Phg). On anchor position P_2 residues NLE, NVA, and 2-AOC resulted in higher-affinity APLs. Unsaturated amino acids propargylglycine (PRG) and allylglycine (ALG) were the best improvements on anchor position P_C.

To understand the factors contributing to enhanced HLA affinity at the molecular level, we solved the crystal structure of HLA-A*02:01 loaded with the CPL [am-phg][NVA]AGIGILT[PRG]. The structure was solved at 1.65-Å resolution (Fig. 2A) and contains two copies of the HLA-A*02:01-peptide complex in the asymmetric unit. Comparison of this structure with the existing structure of HLA-A*02:01 bound to the ELAGIGILTV Mart-1 variant peptide (RCSB Protein Data Bank identification code 1JF1)[44] reveals that both peptides assume a similar overall structure (root mean square deviation of nine peptide Ca atoms is 0.127 Å; Fig. 2B). In addition, no striking differences are observed in the presumed TCR interacting region of the peptides (Ile4-Leu7; Fig. 2B). On P_1 the aromatic residue of am-phg, locked in the D-orientation, shows both a favorable aromatic π-π interaction with Trp167 and a cation-π interaction with the side chain of Lys66 of the HLA a2 domain, whereas the am-phg NH_2-group maintains strong H-bonding interactions with Tyr7 and Tyr171 (Fig. 2C). The contribution of aromatic-π interactions to the binding of peptide and MHC heavy chain has been described previously, in particular the effect of an APL harboring a proline substitution at P_3 in which CH-π interactions between this proline and Tyr159 are

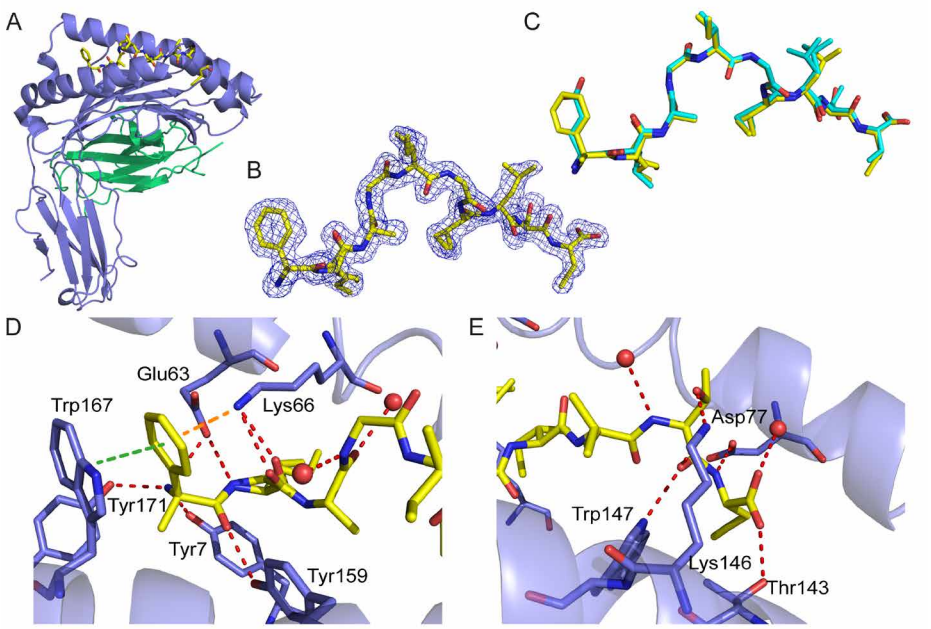

Figure 2. **The crystal structure of HLA-A*0201 loaded with a CPL reveals enhanced protein ligand interactions.** (A) The crystal structure of HLA-A*02:01::[am-phg][NVA]AGIGILT[PRG] was solved at 1.65 Å (RCSB Protein Data Bank identification code 4WJ5). The α- and β2m-chains are illustrated in blue and green, respectively. Peptide [am-phg][NVA]AGIGILT[PRG] is represented as sticks, with carbons in yellow, nitrogen in blue, and oxygen in red. (B) Peptide [am-phg][NVA]AGIGILT[PRG] represented as in (A) together with the final 2mFo-DFc electron density map (blue) displayed at a contour level of 1.0s and a radius of 1.5 Å around the peptide. (C) Overlay of the CPL shown in the same orientation as in (A) with the parent epitope ELAGIGILTV (RCSB Protein Data Bank identification code 1JF1)[35] in cyan. (D) Hydrogen bonding (red dotted lines), π-π interactions (green dotted line), and cation-π interactions (orange dotted line) explain the strong interaction of substituted residues D-am-phg on P_1 and L-NVA on P_2 with HLA-A*02:01. The NVA residue on P_2 protrudes into the hydrophobic P_2 anchor pocket. Water molecules are represented as red spheres. (E) Hydrogen bonding network of the C-terminal part of the CPL with the HLA-A*02:01 α-chain.

noteworthy to mention, as these interactions have been shown to increase the binding affinity significantly between H-2D^b and peptide[45] and to enhance the stability of the H-2D^b::peptide complex[46]. The NVA residue on P_2 protrudes into the hydrophobic anchor pocket and shows two different conformations in one of the peptides of the asymmetric unit, suggesting some degree of flexibility upon interaction with HLA-A*02:01. The NVA residue could stabilize the interaction between peptide and HLA-A*02:01 via van der Waals contact, but also via CH-π interactions with Tyr7, similar to the CH-π interactions reported between proline at P_3 and Tyr159 within the H-2Db::peptide complex[45,46]. The side chain of the PRG residue on P_C fits well into the hydrophobic F-pocket, whereas the main chain atoms form hydrogen bonds with Asp77, Thr143, and a water molecule (Fig. 2D).

Optimized melanoma epitopes are immunogenic and show prolonged activation of CTLs

To test whether CPLs maintained the ability to interact with TCRs, we used these CPLs in pMHC multimer staining experiments. We confirmed that the pMHC multimers loaded with optimized melanoma Ags (e.g., [am-phg][NVA]AGIGILT[PRG]) stained melanoma patient-derived CTLs as efficiently as pMHC multimers charged with the native epitope or with the A2L variant (Fig. 3A). To test the recognition of CPLs by CTLs, TAP-deficient T2 cells were pulsed with EAAGIGILTV-based CPLs and were incubated with HLA-A*02:01^{+} melanoma patient-derived CTLs at various time points. We monitored IFN-γ production as a marker for T cell activation; 48 h after pulsing with CPLs, the APCs were still able to elicit a strong CTL response (Fig. 3B), whereas APCs pulsed with either native EAAGIGILTV epitope or the A2L variant had lost or started losing this ability already after 24 h (Fig. 3C, Table 2). A similar trend was observed for CPLs based on the melanoma Trp-2$_{180\text{-}188}$ epitope SVYDFFVWL (Table 2). To test whether these CPLs are able to elicit an enhanced immune response in vivo, we vaccinated groups of HLA-A*02:01-transgenic mice with optimized Mart-1$_{26\text{-}35}$ and MAGE-C2$_{191\text{-}200}$[47] melanoma epitopes, and we monitored the vaccination-induced T cell frequencies by pMHC multimer staining. Vaccination with enhanced Mart-1 epitope, [am-phg][NVA]AGIGILT[PRG], induced higher frequencies of ELAGIGILTV reactive CTLs, also after a secondary vaccination at day 97 (Fig. 3D). Mice vaccinated with modified Mage-C2$_{191\text{-}200}$ epitope, [Phg][2-AOC]FGLALIEV (Table 2), produced more Mage-C2$_{191\text{-}200}$-reactive CTLs than did those vaccinated with the native epitope at all time points measured.

Selection of optimally modified mHag UTA2-1 peptides

To translate our findings to clinical applications, we proceeded with the optimization of minor histocompatibility Ag (mHag) UTA2-1, QLLNSVLTL[36]. This HLA-A*02:01-restricted epitope was modified and tested in a similar manner as the viral and melanoma peptides. Of 288 CPLs screened, 13 were selected for further analysis and showed—to various degrees—enhanced HLA binding and stability compared with the wild-type peptide (Fig. 4A). This set of CPLs was subsequently screened for recognition by the UTA2-1-specific CTL clone 503A1. Although several CPLs displayed a similar or even decreased CTL activation score compared with the wild-type peptide, CPLs 8 and 9 induced a CTL response at concentrations that were two orders of magnitude lower, indicating improved Ag presentation and recognition (Fig. 4A). These two peptides and a modified peptide that induced equal levels of CTL stimulation, CPL 5, were selected and subjected to further analysis to evaluate their immunogenic properties.

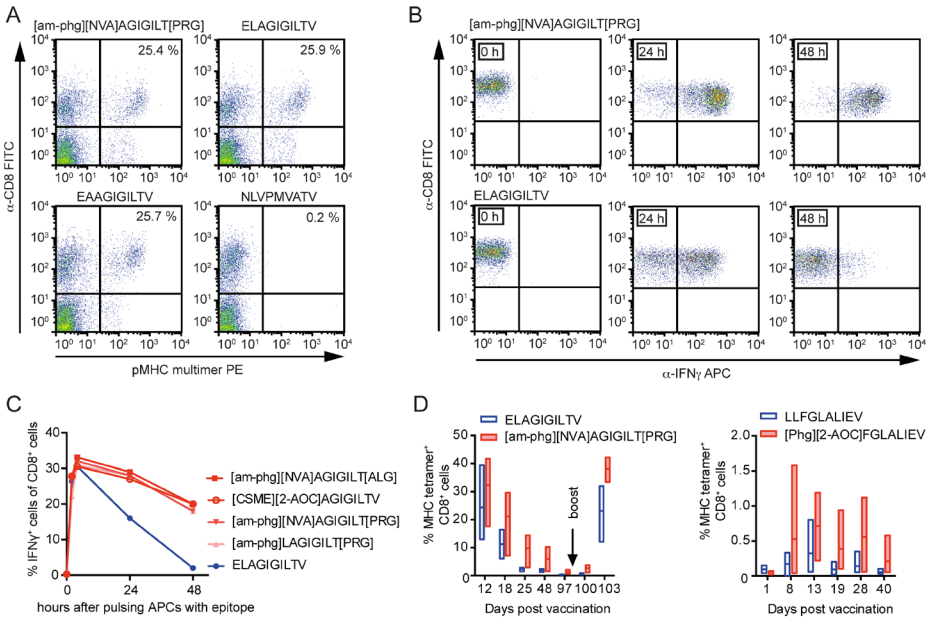

Figure 3. **CPLs are functional Ags and show prolonged activation of CTLs.** (A) Flow cytometry plots showing CTLs from HLA-A*02:01+ melanoma patients stained with pMHC exchange multimers loaded with the indicated tumor-associated Mart-$1_{26–35}$ Ag EAAGIGILTV or synthetic derivatives thereof and viral Ag NLVPMVATV as a negative control. CTLs were stained with anti-CD8-APC Ab and PE-conjugated pMHC multimers. Numbers indicate frequencies of pMHC multimer+ cells among CD8+ cells. (B) Coincubation of EAAGIGILTV specific clonal CTLs with APCs pulsed with a CPL show prolonged CTL activation (IFN-γ response) compared with the heteroclitic tumor-Ag ELAGIGILTV. (C) A time course of stimulation of EAAGIGILTV specific CTLs upon coincubation with APCs pulsed with 50 pM of the indicated peptides. (D) Enhanced T cell responses of HLA-A*02:01-transgenic mice vaccinated with CPLs. Groups of three (left panel) or four (right panel) mice were vaccinated with 100 mg of the indicated peptides, and at the indicated time points peripheral blood was drawn and analyzed by pMHC multimer staining with pMHC multimers presenting ELAGIGILTV (left panel) or LLFGLALIEV (right panel). At day 97, mice in the left panel were administered a secondary vaccination (boost).

Increased efficiency of in vitro and in vivo CTL induction with optimized UTA2-1 epitopes

To evaluate the immunogenicity of CPLs 5, 8, and 9, we first performed in vitro CTL induction experiments in which unprimed PBMCs from two healthy UTA2-1-negative donors were stimulated with these peptides. From 2 to 3 weeks after the first peptide stimulation, increased efficiency of UTA2-1-specific T cell proliferation was seen for CPLs 8 and 9, as measured with pMHC multimer staining (Fig. 4B). The responses were most pronounced for CPL 8. Most importantly, virtually all UTA2-1-specific T cells stained double-positive for the wild-type UTA2-1 tetramer and the modified peptide-specific tetramer, indicating that the induced TCRs

were cross-reactive to both the CPL and the native Ag (Fig. 4B and Fig. S2). This finding was confirmed in an in vivo immunization model in which we immunized HLA-A*02:01-transgenic mice with CPL 8, CPL 9, or the wild-type UTA2-1 peptide. Splenocytes of the immunized mice were analyzed using an IFN-γ ELISPOT assay after stimulation of these cells with naturally mHag UTA2-1-positive and -negative human EBV-LCLs, in some cases exogenously loaded with the CPLs as positive controls. This analysis revealed that CPL 8 induced significantly higher frequencies of immunized peptide-specific CTLs than the wild-type epitope did, and a similar but nonsignificant trend was seen for CPL 9 (Fig. 4C, left panel). Furthermore, both 8- and 9-reactive CTLs were also directed at the natural UTA2-1 epitope presented on the cell surface of $mHag^+$ EBV-LCLs, which was for 8-reactive CTLs a significantly higher number than for the wild-type peptide (Fig. 4C, right panel). Finally, we evaluated whether the T cell responses induced with these CPLs had also retained their cytolytic function against human malignant targets expressing the natural Ag. Therefore, a bioluminescence cytotoxicity assay was performed; it demonstrated that splenocytes from all mice immunized with the UTA2-1 peptide or one of the modified derivatives specifically lysed MM cells endogenously expressing UTA2-1 (Fig. 4D). In contrast, splenocytes from a mouse immunized with an irrelevant peptide not expressed by MM cells did not display any specific lysis of these MM cells, but even stimulated their growth, as is often the result of secreted stimulatory cytokines.

Discussion

The introduction of non-proteogenic amino acids into peptide-based vaccines in principle opens up new avenues for improvement of vaccine delivery and for rational design of epitope vaccines. In this study, we have performed a systematic survey of the structural requirements for peptide binding to the HLA-A*02:01 allele to enhance peptide-MHC affinity, while retaining the ability to activate CTLs by interaction with the TCR. Our approach consisted of the introduction of non-proteogenic, synthetic amino acids into known epitopes at positions close to the N and C termini. Although substitutions with proteogenic amino acids already led to an enhancement of MHC affinity, the introduction of non-proteogenic, synthetic amino acid residues further boosted an increase in affinity. By scanning more than 90 aa residues through a multitude of epitopes, we were able to distill a list of preferred residues that typically lead to improved HLA-A*02:01-binding peptides (Fig. 1B). Notably, substitutions on P_1 with aromatic amino acids in the D conformation (e.g., α,α di-substituted α amino acid am-phg) proved to be favorable. These substitutions induce a gain in HLA affinity that can be explained by the π-π and cation-π interactions of the aromatic ring as well

as the formation of a strong hydrogen bonding network between the NH_2 group and the HLA α-chain, as revealed by the crystal structure of Mart-1-based CPL [am-phg][NVA]AGIGILT[PRG] in complex with HLA-A*02:01 (Fig. 2C). The affinity can be improved further when these replacements at P_1 are combined with NLE, NVA, 2-AOC, and CpAla substitutions at P_2 (Table 2). These residues contain extended alkyl chains that fit into a hydrophobic pocket of the HLA peptide-binding groove. For P_2-monosubstituted variants of Mart-1 peptide EAAGIGILTV HLA binding, scores increase upon extension of the aliphatic side chain in the following order: Ala (18%), NVA (54%), Leu (58%), NLE (59%), and 2-AOC (67%). This result can be explained by more hydrophobic contact between the large alkyl side chains and HLA-A*02:01 residues forming the pocket. In addition, CH-π interactions between the alkyl chains and Tyr7 could contribute to enhanced affinity, similar to those reported for Pro at P_3 and Tyr159 within H-2D^b::peptide structures[46]. However, we cannot exclude that extension of the P_2 side chain beyond that of NVA also affects the overall conformation of the peptide or TCR interaction, as has been shown for other APLs harboring P_2 or P_3 substitutions (see Fig. S3 for a structural analysis of P_2 and P_3 mutations and their modulatory effect on peptide conformation and TCR interaction). Although substitutions on P_3 have been shown to stabilize peptide-MHC interactions and even enhance immunogenicity (this study and Refs. 20, 45, 46), modifying the P_3 position of HLA-A*02:01-restricted epitopes should be performed with caution as this can also lead to loss of immunogenicity (this study and Ref. 48). Incorporation of unsaturated amino acids (PRG and ALG) on anchor position P_C also contributes to enhanced HLA affinity to some extent. C-terminal modification may be of particular value in improving protease resistance of peptide vaccines.

In proof-of-concept studies using T cell activation assays, we showed that several chemically optimized melanoma epitopes indeed resulted in higher and more persistent T cell responses in vitro. Peptide vaccination studies in HLA-A*02:01-transgenic mice with two enhanced melanoma epitopes showed that CTL frequencies were higher and longer lasting than for vaccination with wild-type peptides. These results indicate that the affinity of the peptide for MHC may be a crucial factor in enhanced T cell activation. This greater immunogenic potential can be explained by improved stability of the pMHC complex itself (and hence prolonged lifetime) or by increased stability of the pMHC-TCR complex resulting in extended stimulation of T cells. Although consistent improvements were found in HLA binding, T cell recognition of CPLs differed to some extent from peptide to peptide for all tested modifications, indicating that for each newly selected epitope HLA binding and T cell recognition experiments must be performed before introducing the CPLs to clinical applications.

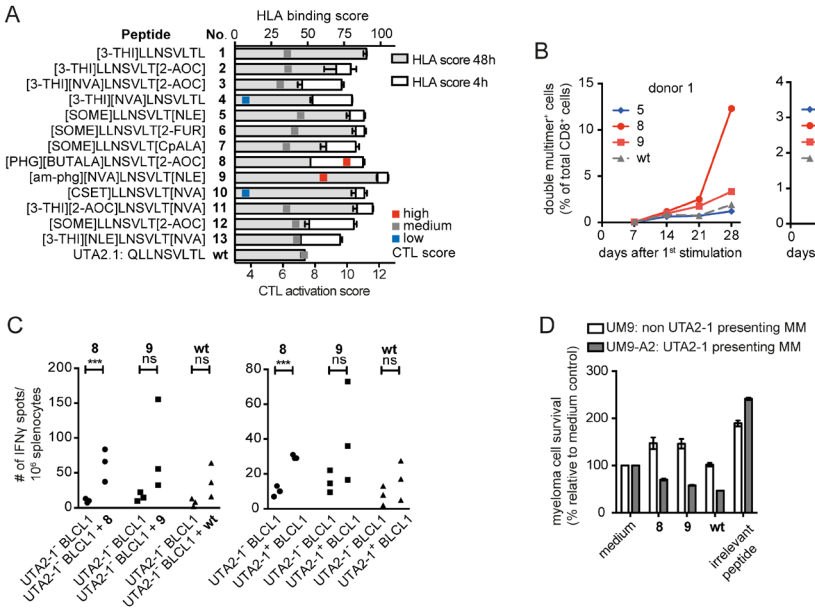

Figure 4. **CPLs of mHag UTA2-1 yield higher CTL frequencies.** (A) In all 13 modifications of the UTA2-1 epitope, an increased HLA-A*02:01 affinity was demonstrated indicated by high HLA binding scores (as in Fig. 1C), in most cases persisting up to 48 h. Coincubating the UTA2-1-specific CTL clone 503A1 together with APCs loaded with these peptides leads to CTL activation, as measured by IFN-γ release. The CTL activation score is the negative logarithm of the half-maximal effective peptide concentration (pEC50) inducing IFN-γ release; these values are representative for three experiments with comparable results. (B) In an in vitro CTL induction experiment, unprimed PBMCs from two UTA2-1$^-$ healthy donors were repeatedly stimulated with one of CPLs 5, 8, or 9 or wild-type (wt) UTA2-1. The proliferation of UTA2-1-specific T cells is strongest for CPL 8 and to a lesser extent for CPL 9, indicating increased efficiency of CTL induction compared with wt peptide, and these induced T cells largely stain double positive for the native UTA2-1 pMHC multimers and the modification-specific pMHC multimers used (Fig. S2). (C) Also in an in vivo immunization experiment with 8, 9, and the wild-type UTA2-1, the induction of Ag-specific cells, as measured by IFN-γ ELISPOT, was most efficient for 8 with significant increases in specific T cell responses against both 8 peptide-loaded and native mHag$^+$ APCs compared with mHag$^-$ APCs. With 9 and wt also specific responses were induced; however, this increase was not significant (ns) as determined with an unpaired t test. Human EBV-LCLs (BLCL1) were used as target APCs. Each replicate depicts the mean of results for every target per mouse, and each target was at least tested in duplicates. (D) The splenocytes from the mice immunized with 8, 9, or wt peptide all lysed UTA2-1 presenting MM cells in a bioluminescence cytotoxicity assay, confirming recognition of the native UTA2-1 Ag and cytotoxic potential of the induced immune response. UM9-A2 is the UTA2-1$^+$ HLA-A*02$^-$ MM cell line UM9 transduced with HLA-A*02:01.

After establishing this basic knowledge, we used the developed toolbox of preferred non-proteogenic amino acids to optimize the minor histocompatibility Ag UTA2-1, which is derived from a polymorphic region of a hematopoietic-specific protein encoded by the biallelic gene C12orf35[36]. Such polymorphic allopeptides, which are exclusively expressed on hematopoietic cells, are generally acknowledged to be ideal targets to induce graft-versus-tumor effects against hematologic tumors after allogeneic stem cell transplantation, without increasing the risk of graft-versus-host disease. For this type of non-self-antigen to which the TCR repertoire has not been negatively selected, further improvement of the immunogenicity is expected to induce antitumor responses that are even more effective. The concept of chemically altered peptides for vaccination is directly translatable to clinical applications using mHags, as the feasibility and effectiveness of dendritic cell vaccination-based immunotherapy for a number of these Ags are currently being evaluated in the clinic. In this study, we show that CPLs based on UTA2-1 can be generated that are capable of inducing an accelerated increase in frequencies of Ag-specific T cells in both in vitro and in vivo models with retained strong cytolytic potential. As such, these CPLs can be used for ex vivo enrichment and faster expansion of Ag-specific T cells for transfer into patients. Evaluation of MHC-peptide recognition by available Ag-specific T cell clones proved important for the strategy described here.

In summary, the present examples show that CPLs display enhanced MHC binding affinity and show a stronger and prolonged capacity to induce T cell activation and proliferation at concentrations lower than their respective wild-types. We have demonstrated that these results can be achieved for virtually any given epitope with a relatively small toolbox of non-proteogenic amino acids. As we increase the number of chemically immuno-optimized epitopes with this strategy, we can now explore the opportunities for clinical applications. Furthermore, a follow-up study, in which additional non-proteogenic amino acids are included that are based on our results, should lead to a more targeted approach in future efforts to improve T cell responses to CPL-based vaccines and to improve the solubility and (metabolic) stability of vaccine candidates.

Materials and Methods

Cells

EBV-transformed B cells (EBV-LCL) from individuals from a Caucasian population in the HapMap database (CEU) as well as multiple myeloma (MM) cell lines U266, UM9 and UM9-A2 (an HLA-A*02:01-transduced variant of UM9) were cultured in RPMI 1640 medium (Invitrogen, Carlsbad, CA) supplemented with 10% FBS

(Integro, Zaandam, the Netherlands) and standard antibiotics (1% penicillin/streptomycin). UTA2-1-specific T cell clone 503A1 was isolated, characterized, and cultured as described previously[36]. PBMCs for the CTL induction experiments were obtained from anonymous HLA-A*02:01^{+}UTA2-1^{-} healthy donors via Sanquin Blood Bank, the Netherlands. Other PBMC samples were obtained from healthy individuals or from patients with stage IV melanoma in accordance with local guidelines, and following informed consent. Ag-specific CD8^{+} T cell clones were generated as described elsewhere[49].

Peptide synthesis, building block synthesis, and resin loading with non-proteogenic amino acids

Peptides were synthesized in house by solid phase peptide synthesis on Multisyntech SYRO I and II peptide synthesizers. The 20 standard proteogenic amino acids (L- and D-forms) were purchased from NovaBiochem. Non-proteogenic amino acids were purchased from different suppliers, provided by Chiralix B.V., or synthesized in house.

Functionalization of solid-phase peptide synthesis resin

Where designated on the C terminus of a peptide, non-proteogenic amino acids were coupled to resin. To 1 g Tentagel S PHB resin (Rapp Polymere, substitution factor 0.27 mmol/g), 2.5 molar equivalents of amino acid were added, mixed, and taken up in 1:1 dichloromethane (Sigma-Aldrich) and N-methyl-2-pyrrolidone (Biosolve); 2.5 molar equivalents of 2,6-dicholorobenzoylchloride (Sigma-Aldrich) and 8.5 molar equivalents of pyridine (Sigma-Aldrich) were added, and the resulting solution was mixed by nitrogen flow and shaken overnight at room temperature.

Peptide binding and stability

HLA binding affinity of peptides was determined by a fluorescence polarization (FP) assay[38] based on ultraviolet-mediated MHC peptide exchange methodology[50]. Purified soluble MHC class I complexes (HLA-A*02:01) were loaded with an ultraviolet-labile peptide KILGFVFJV, in which J is photocleavable 3-amino-3-(2-nitrophenyl) propionic acid. MHC molecules were diluted in PBS supplemented with 0.5 mg/ml b-g-globulin (Sigma-Aldrich) to a final concentration of 0.75 mM and pipetted into a 96-well microplate. Tracer peptide FLPSDCFPSV (based on FLPSDFFPSV, Hepatitis B virus core protein$_{(18\text{-}27)}$) with a fluorescent TAMRA molecule covalently bound to the cysteine residue through a maleimide linkage was used as the competitor peptide[40]. This tracer peptide was diluted in PBS/b-g-globulin to a concentration of 6 nM and pipetted into a 96-well microplate. The peptides of interest were diluted in DMSO to a concentration of 125 mM and added to a 96-well microplate. The samples were prepared using a Hamilton high-throughput

liquid-handling robot at final concentrations of 0.5 mM MHC, 1 nM tracer, and 4.2 mM peptide in 30 ml together into a Corning black nonbinding surface 384-well microplate. The 384-well microplate was placed under a ultraviolet lamp (350 nm) for 30 min at 4°C to cleave the ultraviolet-labile peptide. The plate was then analyzed using a PerkinElmer Envision or BMG PHERAstar plate reader. FP values in millipolarization units were normalized to an HLA binding score that is defined as the percentage inhibition of fluorescent tracer peptide binding relative to control (100 mM of FLPSDFFPSV). Instant JChem (version 5.9, 2012) and the JChem for Excel plug-in were used for structure database management (ChemAxon, Budapest, Hungary). The percentage inhibition values of serial peptide dilutions were then used to calculate the IC50 values of peptide binding. Data were plotted in GraphPad Prism 5.01 and IC50 curves were fitted using the nonlinear regression sigmoidal dose-response formula.

Crystallization

HLA molecules were expressed and refolded as described[51] in the presence of peptide ([am-phg][NVA]AGIGILT[PRG], in which am-phg is D-alpha-methyl-phenylglycine, NVA is norvaline and PRG is propargylglycine). Subsequently, pMHC complexes were loaded on a Mono-Q anion exchange column and eluted with NaCl gradient in 20 mM Tris•Cl (pH 7.0). Complexes were further purified with gel-filtration chromatography on a Phenomex BioSep SEC-s3000 column in 20 mM Tris•Cl (pH 7.0) and 150 mM NaCl, followed by a final purification step on the Mono-Q anion exchange column and elution with NaCl gradient in 20 mM Tris•Cl (pH 7.0). Protein buffer was exchanged to 20 mM MES (pH 6.5) using a Centriprep concentrator, and final preparations were flash-frozen in liquid nitrogen and stored at 280°C. Crystals were generated essentially as described[52]. Briefly, crystals were grown from 22-24% PEG 1500, 0.1 M MES (adjusted to pH 6.5 with NaOH) using microseeding in 4-ml hanging drops (2 ml protein + 2 ml crystallization solution) at 20°C. Crystals were frozen in 30% PEG 1500, 12% glycerol, and 0.1 M MESNaOH (pH 6.5). Crystals were mounted in loops, vitrified in liquid nitrogen, and stored until data collection.

X-ray data collection and structure refinement

X-ray diffraction data for a single HLA-2.1::[am-phg][NVA]AGIGILT[PRG] crystal were collected at beamline PX3 at the Swiss Light Source (illigen, Switserland) at 100 K at a wavelength of 0.97890 Å. Data were processed using XDS[53] and integrated with SCALA[54] within the CCP4 suite[55]. A molecular replacement solution was obtained with AMORE[56] using the structure of HLA-A*02:01::ELAGIGILTV (RCSB Protein Data Bank identification code 1JF1 [http://www.rcsb.org/structure/1jf1])[44] as the search model. The structure was refined during multiple cycles of manual building and refinement using the Refinement of Macromolecular Structures

by the Maximum-Likelihood method[57]. A final refinement and evaluation was performed using the PDB_REDO webserver[58]. The final structure was resolved at 1.65 Å with R/R_{free} of 15.5/17.9%. Ninety-seven percent of the residues are within favorable regions of the Ramachandran plot, whereas 3% are within allowed regions. Rmsd values for bond lengths and angles are 0.012 Å and 1.563 Å, respectively. Data collection and refinement statistics are summarized in Table 1. The crystal structure presented in this article has been submitted to the RCSB Protein Data Bank (http://www.rcsb.org/pdb/home/home.do) under identification code 4WJ5.

T cell staining and flow cytometry

T cell staining with exchange pMHC multimers was performed essentially as described[51]. Enhanced and control peptides in DMSO were added to biotinylated MHC monomers (25 mg/ml in PBS) to a final concentration of 50 mM and ultraviolet irradiated for 30 min. Samples were left at room temperature for an additional 30 min. Subsequently, the plates were centrifuged for 5 min at 3300 × *g* to remove disintegrated MHC molecules. Streptavidin-R-PE (Life Technologies) was added to the exchanged monomers to a final concentration of 13.5 mg/ml. Resulting pMHC multimer (2 ml) was added to 100,000 T cells and incubated for 15 min at 37°C. Samples were stained with 1 ml APC Mouse Anti-Human CD8 (BD Pharmingen) and incubated for 20 min on ice. Subsequently, after two wash steps with PBS, samples were taken up in FACS buffer (0.5% BSA, 0.02% sodium azide in PBS) containing 1% propidium iodide to distinguish between live and dead T cells in the FACS analysis. Peptide-MHC binding to TCRs was analyzed by flow cytometry on either a Beckman Coulter CyAn ADP Analyzer or a BD FACSCalibur machine. Data were analyzed using FlowJo 7.6.1 (Tree Star) and Microsoft Excel 2007.

Intracellular IFN-γ staining

T cell activation assays based on IFN-γ secretion were performed using a BD Cytofix/Cytoperm fixation/permeabilization solution kit with BD GolgiPlug. To enable the immediate and sustained presentation of peptides to established T cell clones, 50,000 T2 APCs were pulsed with serial dilutions of the peptides for 1 h at 37°C in assay medium (100 ml RPMI/10% FCS) in a 96-well plate. After removing unbound peptides by centrifugation at 600 × *g* for 3 min, the peptide-pulsed T2 cells were cocultured with T cell clones (50,000 T cells per well in 100 ml assay medium supplemented with 1 ml/ml; BD GolgiPlug). Alternatively, to measure prolonged peptide presentation, peptide-pulsed T2 cells were incubated for an additional 23 or 47 h in 100 ml medium alone before incubation with T cells. After the addition of T cells, plates were centrifuged at 100 × *g* for 2 min to facilitate APC-T cell contacts. Positive controls included T cells stimulated

only with phorbol 12-myristate 13-acetate (PMA; 0.05 mg/ml) and ionomycin (1 mg/ml) in 100 ml medium. After 4 h of incubation at 37°C, plates were spun at 600 × *g* for 3 min, medium was discarded, and the cells were resuspended in 50 ml FACS buffer with FITCCD8 Ab (20 ml/ml) for 15 min in the dark at room temperature. After two spin (800 × *g* for 3 min) and wash steps with 200 ml FACS buffer cells were resuspended in 100 ml Cytofix/Cytoperm solution and incubated on ice for 20 min. The cells were then spin-washed twice with 200 ml Perm/Wash buffer and resuspended in 50 ml Perm/Wash buffer containing 20 ml/ml APC-IFN-γ Ab to incubate on ice for 30 min. After a final spin-wash with 200 ml of perm/wash buffer, cells were resuspended in FACS buffer and measured on a Beckman Coulter CyAn ADP Analyzer. Data were analyzed using FlowJo 7.6.1 (Tree Star) and Microsoft Excel 2007.

ELISA

T cell lines or clones were incubated for 20-24 h with HLA-A*02:01$^+$ UTA2-12 EBV-LCL lines pulsed with the tested peptides for 3 h at 37°C in culture medium as described elsewhere[36]. The IFN-γ content of cell-free supernatants was determined using a commercial ELISA kit (Pelipair, Sanquin) according to the manufacturer's instructions.

In vitro CTL inductions

PBMCs from HLA-A*02:01$^+$UTA2-1$^-$ healthy donors were sorted on CD8 expression by MACS following the instructions of the manufacturer (Miltenyi Biotec, Bergisch Gladbach, Germany). The CD8$^+$ fraction was used as effector cells; they were stimulated once weekly by either the CD82 fraction or bulk PBMCs pulsed for 3 hours with either one of the modified peptides or the wild-type UTA2-1 peptide and irradiated at 2500 rad. Culture medium was RPMI 1640 supplemented with 10% HS and antibiotics, rhuIL-2 was added twice a week starting from day 5. pMHC multimer staining was performed weekly, preceding each stimulation.

Bioluminescence-based cytotoxicity assays

Murine splenocytes were incubated for 20-24 h with luciferase-transduced MM cell lines in white, opaque, flat-bottom 96-well plates (Costar). After the addition of 125 mg/ml beetle luciferin, the light signal emitted from surviving multiple myeloma cells was determined using a luminometer (SpectraMax; Molecular Devices, Sunnyvale, CA). The percentage survival of MM cells was calculated using the following formula: Relative cell survival = 100% × (Experimental luciferase signal / Medium control luciferase signal).

Mouse immunizations

HLA-A*02:01 transgenic mice also containing a human CD8 binding domain (The Jackson Laboratory, Bar Harbor, ME) were injected i.v. at both sides of the tail base with 1-100 mg peptide and 50 mg CpG oligonucleotides 1826, emulsified in IFA, as adapted from Li et al.[59]. One-hundred microliters of blood was collected from the tail-tip at several time points and was analyzed for the presence of epitope-specific T cells by flow cytometry directly after collection. PE- and APC-labeled pMHC multimers containing the wild-type epitope were generated for this purpose, and 2 ml of PE-multimers and 4 ml of APC-multimers were used for dual staining of the blood samples. Prior to staining, all blood samples were erylysed.

Alternatively, for the UTA2-1 modifications and wild-type peptide, at the end of the experiment, spleens from all mice were isolated and analyzed for specific T cell responses using a commercial IFN-γ ELISPOT kit (Sanquin, Amsterdam, the Netherlands). Human EBV-LCLs either expressing or not expressing mHag UTA2-1, or exogenously loaded with one of the peptides, were used as target cells. Three mice were immunized with each peptide.

Online supplemental material

Figure S1. Affinity screening data of viral and melanoma epitope based CPLs.
Figure S2. T cells induced with CPLs are cross-reactive to pMHC multimers charged with native mHag or CPL.
Figure S3. Peptide substitutions at P_2 and P_3 modulate peptide-HLA-A*02:01 interaction and/or TCR binding.
Table S1. Peptide HLA binding scores of viral epitopes containing substitutions with proteogenic amino acids (single letter code).

Acknowledgements

We thank Henk Hilkmann and Dris El Atmioui for peptide synthesis, Dr. Carsten Linnemann for help with the modified melanoma peptide vaccination studies, beamline scientists at the Swiss Light Source (Villigen, Switzerland) for assistance during data collection experiments, and Robbie Joosten for advice with PDB_REDO and structural analysis. The authors have no financial conflicts of interest.

References

1. Hodi, F. S., S. J. O'Day, D. F. McDermott, R. W. Weber, J. A. Sosman, J. B. Haanen, R. Gonzalez, C. Robert, D. Schadendorf, J. C. Hassel, et al. 2010. Improved survival with ipilimumab in patients with metastatic melanoma. N. Engl. J. Med. 363: 711-723.
2. Rosenberg, S. A., J. C. Yang, and N. P. Restifo. 2004. Cancer immunotherapy: moving beyond current vaccines. Nat. Med. 10: 909-915.
3. Slansky, J. E., F. M. Rattis, L. F. Boyd, T. Fahmy, E. M. Jaffee, J. P. Schneck, D. H. Margulies, and D. M. Pardoll. 2000. Enhanced antigen-specific antitumor immunity with altered peptide ligands that stabilize the MHC-peptide-TCR complex. Immunity 13: 529-538.
4. Tang, Y., Z. Lin, B. Ni, J. Wei, J. Han, H. Wang, and Y. Wu. 2007. An altered peptide ligand for naı¨ve cytotoxic T lymphocyte epitope of TRP-2(180-188) enhanced immunogenicity. Cancer Immunol. Immunother. 56: 319-329.
5. Bowerman, N. A., L. A. Colf, K. C. Garcia, and D. M. Kranz. 2009. Different strategies adopted by K(b) and L(d) to generate T cell specificity directed against their respective bound peptides. J. Biol. Chem. 284: 32551-32561.
6. Engels, B., V. H. Engelhard, J. Sidney, A. Sette, D. C. Binder, R. B. Liu, D. M. Kranz, S. C. Meredith, D. A. Rowley, and H. Schreiber. 2013. Relapse or eradication of cancer is predicted by peptide-major histocompatibility complex affinity. Cancer Cell 23: 516-526.
7. Moutaftsi, M., S. Salek-Ardakani, M. Croft, B. Peters, J. Sidney, H. Grey, and A. Sette. 2009. Correlates of protection efficacy induced by vaccinia virusspecific $CD8^+$ T-cell epitopes in the murine intranasal challenge model. Eur. J. Immunol. 39: 717-722.
8. Van der Burg, S. H., M. J. Visseren, R. M. Brandt, W. M. Kast, and C. J. Melief. 1996. Immunogenicity of peptides bound to MHC class I molecules depends on the MHC-peptide complex stability. J. Immunol. 156: 3308-3314.
9. Yu, Z., M. R. Theoret, C. E. Touloukian, D. R. Surman, S. C. Garman, L. Feigenbaum, T. K. Baxter, B. M. Baker, and N. P. Restifo. 2004. Poor immunogenicity of a self/tumor antigen derives from peptide-MHC-I instability and is independent of tolerance. J. Clin. Invest. 114: 551-559.
10. Rudolph, M. G., R. L. Stanfield, and I. A. Wilson. 2006. How TCRs bind MHCs, peptides, and coreceptors. Annu. Rev. Immunol. 24: 419-466.
11. Evavold, B. D., J. Sloan-Lancaster, and P. M. Allen. 1993. Tickling the TCR: selective T-cell functions stimulated by altered peptide ligands. Immunol. Today 14: 602-609.
12. Valmori, D., J. F. Fonteneau, C. M. Lizana, N. Gervois, D. Lie´nard, D. Rimoldi, V. Jongeneel, F. Jotereau, J. C. Cerottini, and P. Romero. 1998. Enhanced generation of specific tumor-reactive CTL in vitro by selected Melan-A/MART-1 immunodominant peptide analogues. J. Immunol. 160: 1750-1758.
13. Rammensee, H. G., T. Friede, and S. Stevanoviı´c. 1995. MHC ligands and peptide motifs: first listing. Immunogenetics 41: 178-228.
14. Fremont, D. H., M. Matsumura, E. A. Stura, P. A. Peterson, and I. A. Wilson. 1992. Crystal structures of two viral peptides in complex with murine MHC class I H-2Kb. Science 257: 919-927.
15. Silver, M. L., H. C. Guo, J. L. Strominger, and D. C. Wiley. 1992. Atomic structure of a human MHC molecule presenting an influenza virus peptide. Nature 360: 367-369.
16. Falk, K., O. Ro¨tzschke, S. Stevanovic´, G. Jung, and H. G. Rammensee. 1991. Allele-specific motifs revealed by sequencing of self-peptides eluted from MHC molecules. Nature 351: 290-296.
17. Lee, J. K., G. Stewart-Jones, T. Dong, K. Harlos, K. Di Gleria, L. Dorrell, D. C. Douek, P. A. van der Merwe, E. Y. Jones, and A. J. McMichael. 2004. T cell cross-reactivity and conformational changes during TCR engagement. J. Exp. Med. 200: 1455-1466.
18. Chen, J.-L., G. Stewart-Jones, G. Bossi, N. M. Lissin, L. Wooldridge, E. M. L. Choi, G. Held, P. R. Dunbar, R. M. Esnouf, M. Sami, et al. 2005. Structural and kinetic basis for heightened immunogenicity of T cell vaccines. J. Exp. Med. 201: 1243-1255.
19. Ekeruche-Makinde, J., M. Clement, D. K. Cole, E. S. J. Edwards, K. Ladell, J. J. Miles, K. K. Matthews, A. Fuller, K. A. Lloyd, F. Madura, et al. 2012. T-cell receptor-optimized peptide skewing of the T-cell repertoire can enhance antigen targeting. J. Biol. Chem. 287: 37269-37281.
20. Tangri, S., G. Y. Ishioka, X. Huang, J. Sidney, S. Southwood, J. Fikes, and A. Sette. 2001. Structural features of peptide analogs of human histocompatibility leukocyte antigen class I epitopes that are more potent and immunogenic than wild-type peptide. J. Exp. Med. 194: 833-846.

21. Gladney, K. H., J. Pohling, N. A. Hollett, K. Zipperlen, M. E. Gallant, and M. D. Grant. 2012. Heteroclitic peptides enhance human immunodeficiency virus-specific CD8(+) T cell responses. Vaccine 30: 6997-7004.
22. Douat-Casassus, C., N. Marchand-Geneste, E. Diez, N. Gervois, F. Jotereau, and S. Quideau. 2007. Synthetic anticancer vaccine candidates: rational design of antigenic peptide mimetics that activate tumor-specific T-cells. J. Med. Chem. 50: 1598-1609.
23. Jones, M. A., J. K. Notta, M. Cobbold, M. Palendira, A. D. Hislop, J. Wilkie, and J. S. Snaith. 2008. Synthesis and ex vivo profiling of chemically modified cytomegalovirus CMVpp65 epitopes. J. Pept. Sci. 14: 313-320.
24. Weber, J. S., N. J. Vogelzang, M. S. Ernstoff, O. B. Goodman, L. D. Cranmer, J. L. Marshall, S. Miles, D. Rosario, D. C. Diamond, Z. Qiu, et al. 2011. A phase 1 study of a vaccine targeting preferentially expressed antigen in melanoma and prostate-specific membrane antigen in patients with advanced solid tumors. J. Immunother. 34: 556-567.
25. Liu, L., A. I. Bot, and D. C. Diamond, inventors; Mannkind Corporation, assignee. Peptide analogues. United States patent application 13/481,741, Publication No. US 2013/0017213 A1. 2013 Jan 17.
26. Go´mez-Nun˜ez, M., K. J. Haro, T. Dao, D. Chau, A. Won, S. Escobar-Alvarez, V. Zakhaleva, T. Korontsvit, D. Y. Gin, and D. A. Scheinberg. 2008. Non-natural and photo-reactive amino acids as biochemical probes of immune function. PLoS ONE 3: e3938.
27. Blanchet, J. S., D. Valmori, I. Dufau, M. Ayyoub, C. Nguyen, P. Guillaume, B. Monsarrat, J. C. Cerottini, P. Romero, and J. E. Gairin. 2001. A new generation of Melan-A/MART-1 peptides that fulfill both increased immunogenicity and high resistance to biodegradation: implication for molecular anti-melanoma immunotherapy. J. Immunol. 167: 5852-5861.
28. Webb, A. I., M. A. Dunstone, N. A. Williamson, J. D. Price, A. de Kauwe, W. Chen, A. Oakley, P. Perlmutter, J. McCluskey, M. I. Aguilar, et al. 2005. T cell determinants incorporating beta-amino acid residues are protease resistant and remain immunogenic in vivo. J. Immunol. 175: 3810-3818.
29. Guichard, G., A. Zerbib, F. A. Le Gal, J. Hoebeke, F. Connan, J. Choppin, J. P. Briand, and J. G. Guillet. 2000. Melanoma peptide MART-1(27-35) analogues with enhanced binding capacity to the human class I histocompatibility molecule HLA-A2 by introduction of a beta-amino acid residue: implications for recognition by tumor-infiltrating lymphocytes. J. Med. Chem. 43: 3803-3808.
30. Reinelt, S., M. Marti, S. De´dier, T. Reitinger, G. Folkers, J. A. de Castro, and D. Rognan. 2001. Beta-amino acid scan of a class I major histocompatibility complex-restricted alloreactive T-cell epitope. J. Biol. Chem. 276: 24525-24530.
31. Purcell, A. W., J. McCluskey, and J. Rossjohn. 2007. More than one reason to rethink the use of peptides in vaccine design. Nat. Rev. Drug Discov. 6: 404-414.
32. Guichard, G., F. Connan, R. Graff, M. Ostankovitch, S. Muller, J. G. Guillet, J. Choppin, and J. P. Briand. 1996. Partially modified retro-inverso pseudopeptides as non-natural ligands for the human class I histocompatibility molecule HLA-A2. J. Med. Chem. 39: 2030-2039.
33. Nair, D. T., K. J. Kaur, K. Singh, P. Mukherjee, D. Rajagopal, A. George, V. Bal, S. Rath, K. V. S. Rao, and D. M. Salunke. 2003. Mimicry of native peptide antigens by the corresponding retro-inverso analogs is dependent on their intrinsic structure and interaction propensities. J. Immunol. 170: 1362-1373.
34. Marschütz, M. K., W. Zauner, F. Mattner, A. Otava, M. Buschle, and A. Bernkop-Schnürch. 2002. Improvement of the enzymatic stability of a cytotoxic T-lymphocyte-epitope model peptide for its oral administration. Peptides 23: 1727-1733.
35. McGregor, D. P. 2008. Discovering and improving novel peptide therapeutics. Curr. Opin. Pharmacol. 8: 616-619.
36. Oostvogels, R., M. C. Minnema, M. van Elk, R. M. Spaapen, G. D. te Raa, B. Giovannone, A. Buijs, D. van Baarle, A. P. Kater, M. Griffioen, et al. 2013. Towards effective and safe immunotherapy after allogeneic stem cell transplantation: identification of hematopoietic-specific minor histocompatibility antigen UTA2-1. Leukemia 27: 642-649.
37. Morrison, J., J. Elvin, F. Latron, F. Gotch, R. Moots, J. L. Strominger, and A. McMichael. 1992. Identification of the nonamer peptide from influenza A matrix protein and the role of pockets of HLA-A2 in its recognition by cytotoxic T lymphocytes. Eur. J. Immunol. 22: 903-907.

38. Diamond, D. J., J. York, J. Y. Sun, C. L. Wright, and S. J. Forman. 1997. Development of a candidate HLA A*0201 restricted peptide-based vaccine against human cytomegalovirus infection. Blood 90: 1751-1767.
39. Buchli, R., R. S. VanGundy, H. D. Hickman-Miller, C. F. Giberson, W. Bardet, and W. H. Hildebrand. 2005. Development and validation of a fluorescence polarization-based competitive peptide-binding assay for HLA-A*02:01—a new tool for epitope discovery. Biochemistry 44: 12491-12507.
40. Rodenko, B., M. Toebes, P. H. N. Celie, A. Perrakis, T. N. M. Schumacher, and H. Ovaa. 2009. Class I major histocompatibility complexes loaded by a periodate trigger. J. Am. Chem. Soc. 131: 12305-12313.
41. Kawakami, Y., S. Eliyahu, K. Sakaguchi, P. F. Robbins, L. Rivoltini, J. R. Yannelli, E. Appella, and S. A. Rosenberg. 1994. Identification of the immunodominant peptides of the MART-1 human melanoma antigen recognized by the majority of HLA-A2-restricted tumor infiltrating lymphocytes. J. Exp. Med. 180: 347-352.
42. Parkhurst, M. R., E. B. Fitzgerald, S. Southwood, A. Sette, S. A. Rosenberg, and Y. Kawakami. 1998. Identification of a shared HLA-A*02:01-restricted T-cell epitope from the melanoma antigen tyrosinase-related protein 2 (TRP2). Cancer Res. 58: 4895-4901.
43. Mitchell, M. S., J. Kan-Mitchell, B. Minev, C. Edman, and R. J. Deans. 2000. A novel melanoma gene (MG50) encoding the interleukin 1 receptor antagonist and six epitopes recognized by human cytolytic T lymphocytes. Cancer Res. 60: 6448-6456.
44. Sliz, P., O. Michielin, J. C. Cerottini, I. Luescher, P. Romero, M. Karplus, and D. C. Wiley. 2001. Crystal structures of two closely related but antigenically distinct HLA-A2/melanocyte-melanoma tumor-antigen peptide complexes. J. Immunol. 167: 3276-3284.
45. Van Stipdonk, M. J. B., D. Badia-Martinez, M. Sluijter, R. Offringa, T. van Hall, and A. Achour. 2009. Design of agonistic altered peptides for the robust induction of CTL directed towards H-2Db in complex with the melanoma-associated epitope gp100. Cancer Res. 69: 7784-7792.
46. Uchtenhagen, H., E. T. Abualrous, E. Stahl, E. B. Allerbring, M. Sluijter, M. Zacharias, T. Sandalova, T. van Hall, S. Springer, P.-Å . Nygren, and A. Achour. 2013. Proline substitution independently enhances H-2D(b) complex stabilization and TCR recognition of melanoma-associated peptides. Eur. J. Immunol. 43: 3051-3060.
47. Ma, W., C. Germeau, N. Vigneron, A.-S. Maernoudt, S. Morel, T. Boon, P. G. Coulie, and B. J. Van den Eynde. 2004. Two new tumor-specific antigenic peptides encoded by gene MAGE-C2 and presented to cytolytic T lymphocytes by HLA-A2. Int. J. Cancer 109: 698-702.
48. Martinez-Hackert, E., N. Anikeeva, S. A. Kalams, B. D.Walker,W. A. Hendrickson, and Y. Sykulev. 2006. Structural basis for degenerate recognition of natural HIV peptide variants by cytotoxic lymphocytes. J. Biol. Chem. 281: 20205-20212.
49. Van Buuren, M. M., F. E. Dijkgraaf, C. Linnemann, M. Toebes, C. X. L. Chang, J. Y. Mok, M. Nguyen, W. J. E. van Esch, P. Kvistborg, G. M. Grotenbreg, and T. N. M. Schumacher. 2014. HLA micropolymorphisms strongly affect peptide-MHC multimer-based monitoring of antigen-specific $CD8^+$ T cell responses. J. Immunol. 192: 641-648.
50. Toebes, M., M. Coccoris, A. Bins, B. Rodenko, R. Gomez, N. J. Nieuwkoop, W. van de Kasteele, G. F. Rimmelzwaan, J. B. A. G. Haanen, H. Ovaa, and T. N. M. Schumacher. 2006. Design and use of conditional MHC class I ligands. Nat. Med. 12: 246-251.
51. Toebes, M., B. Rodenko, H. Ovaa, and T. N. M. Schumacher. 2009. Generation of peptide MHC class I monomers and multimers through ligand exchange. Curr. Protoc. Immunol. 18: 18.16.
52. Celie, P. H. N., M. Toebes, B. Rodenko, H. Ovaa, A. Perrakis, and T. N. M. Schumacher. 2009. UV-induced ligand exchange in MHC class I protein crystals. J. Am. Chem. Soc. 131: 12298-12304.
53. Kabsch, W. 2010. XDS. Acta Crystallogr. D Biol. Crystallogr. 66: 125-132.
54. Evans, P. 2006. Scaling and assessment of data quality. Acta Crystallogr. D Biol. Crystallogr. 62: 72-82.
55. Winn, M. D., C. C. Ballard, K. D. Cowtan, E. J. Dodson, P. Emsley, P. R. Evans,R. M. Keegan, E. B. Krissinel, A. G. W. Leslie, A. McCoy, et al. 2011. Overview of the CCP4 suite and current developments. Acta Crystallogr. D Biol. Crystallogr. 67: 235-242.
56. Navaza, J. 1994. AMoRe: an automated package for molecular replacement. Acta Crystollagr. A. 50: 157-163.

57. Murshudov, G. N., A. A. Vagin, and E. J. Dodson. 1997. Refinement of macromolecular structures by the maximum-likelihood method. Acta Crystallogr. D Biol. Crystallogr. 53: 240-255.
58. Joosten, R. P., K. Joosten, S. X. Cohen, G. Vriend, and A. Perrakis. 2011. Automatic rebuilding and optimization of crystallographic structures in the Protein Data Bank. Bioinformatics 27: 3392-3398.
59. Li, L.-P., J. C. Lampert, X. Chen, C. Leitao, J. Popovic, W. Müller, and T. Blankenstein. 2010. Transgenic mice with a diverse human T cell antigen receptor repertoire. Nat. Med. 16: 1029-1034.